Posttranslational stability of the heme biosynthetic enzyme ferrochelatase is dependent on iron availability and intact iron-sulfur cluster assembly machinery

Daniel R. Crooks,[1,2] Manik C. Ghosh,[2] Ronald G. Haller,[3] Wing-Hang Tong,[2] and Tracey A. Rouault[2]

[1]Department of Biochemistry, Molecular and Cellular Biology, Georgetown University Medical Center, Washington, DC; [2]Molecular Medicine Program, *Eunice Kennedy Shriver* National Institute of Child Health and Human Development, Bethesda, MD; and [3]Department of Neurology, University of Texas Southwestern Medical Center and Veterans Administration North Texas Medical Center, and Neuromuscular Center, Institute for Exercise and Environmental Medicine, Dallas

Mammalian ferrochelatase, the terminal enzyme in the heme biosynthetic pathway, possesses an iron-sulfur [2Fe-2S] cluster that does not participate in catalysis. We investigated ferrochelatase expression in iron-deficient erythropoietic tissues of mice lacking iron regulatory protein 2, in iron-deficient murine erythroleukemia cells, and in human patients with ISCU myopathy. Ferrochelatase activity and protein levels were dramatically decreased in *Irp2*$^{-/-}$ spleens, whereas ferrochelatase mRNA levels were increased, demonstrating posttranscriptional regulation of ferrochelatase in vivo. Translation of ferrochelatase mRNA was unchanged in iron-depleted murine erythroleukemia cells, and the stability of mature ferrochelatase protein was also unaffected. However, the stability of newly formed ferrochelatase protein was dramatically decreased during iron deficiency. Ferrochelatase was also severely depleted in muscle biopsies and cultured myoblasts from patients with ISCU myopathy, a disease caused by deficiency of a scaffold protein required for Fe-S cluster assembly. Together, these data suggest that decreased Fe-S cluster availability because of cellular iron depletion or impaired Fe-S cluster assembly causes reduced maturation and stabilization of apoferrochelatase, providing a direct link between Fe-S biogenesis and completion of heme biosynthesis. We propose that decreased heme biosynthesis resulting from impaired Fe-S cluster assembly can contribute to the pathogenesis of diseases caused by defective Fe-S cluster biogenesis. (Blood. 2010;115:860-869)

Introduction

Heme, the iron-containing tetrapyrrole cofactor of hemoproteins, is indispensable for many cellular and organismal metabolic processes because of its ability to confer gas transport and electron transfer functionalities to countless enzymes. In animals, heme biosynthesis begins in the mitochondrion with the conjugation of succinyl-coenzyme A and glycine by δ-aminolevulinic acid synthase (ALAS) to form δ-aminolevulinic acid (ALA).[1] ALA is transported into the cytoplasm where it serves as the building block for the tetrapyrrole macrocycle via a series of well-characterized reactions,[2] and the process is concluded in the mitochondrion with insertion of iron into protoporphyrin IX (PPIX) by ferrochelatase to form heme.[3]

Large amounts of iron and heme are required by developing erythroblasts to supply millimolar quantities of hemoglobin in erythrocytes. An iron-responsive element (IRE) present in the 5′ untranslated region (UTR) of the mRNA that encodes erythroid-specific isoform of ALAS (*Alas2*)[4] allows for binding of iron regulatory proteins 1 and 2 (IRP1/2) during iron deficiency, resulting in decreased synthesis of aminolevulinic acid synthase 2 (ALAS2) protein and restricted initiation of heme biosynthesis. In contrast, IRE sequences in the 3′-UTR of transferrin receptor 1 (*Tfr1*) confer protection from nuclease degradation on IRP binding,[5] thus increasing TfR1 protein expression during iron deficiency. Accordingly, *Irp2*$^{-/-}$ erythroblasts express less TfR1, probably contributing to the low hematocrit and microcytosis observed in these animals despite normal serum transferrin saturation levels.[6,7]

Irp2$^{-/-}$ mice also possess more than 100-fold elevated levels of erythrocyte PPIX,[6] a condition found in patients affected by erythropoietic protoporphyria (EPP). EPP is characterized by elevated erythrocyte PPIX, resulting in painful cutaneous photosensitivity and, infrequently, hepatic failure caused by biliary occlusions of crystalline protoporphyrin.[8] Whereas elevated erythrocyte PPIX levels in *Irp2*$^{-/-}$ mice are associated with the loss of IRP2-mediated translational repression of ALAS2,[6] EPP in humans is usually caused by mutations in the ferrochelatase (*FECH*) gene.[9] EPP patients usually possess less than one-third of the normal level of ferrochelatase activity,[10] which most frequently results from inheritance of a mutated *FECH* allele with decreased activity together with a low-expressing normal *FECH* allele.[11]

Unlike the *Saccharomyces cerevisiae* and *Escherichia coli* enzymes, mammalian ferrochelatase possesses a solvent-exposed [2Fe-2S] cluster.[12,13] Interestingly, replacement of the carboxy-terminal segment of mammalian ferrochelatase containing 3 of the cluster-ligating cysteines with *S cerevisiae* ferrochelatase sequence yielded a non–cluster-containing protein that retained some activity.[14] The crystal structure of human ferrochelatase suggests a structural role for the Fe-S cluster by revealing a unique stabilizing bridge formed by the cluster between the 3 carboxy-terminal cysteines and a fourth internal cysteine.[12,15] Mutations in the 4 coordinating cysteine residues of recombinant human ferrochelatase resulted in an inactive enzyme,[15,16] consistent with observations in 5 EPP patients in which such mutations also resulted in inactive enzyme.[17]

Submitted September 10, 2009; accepted November 1, 2009. Prepublished online as *Blood* First Edition paper, November 25, 2009; DOI 10.1182/blood-2009-09-243105.

The publication costs of this article were defrayed in part by page charge payment. Therefore, and solely to indicate this fact, this article is hereby marked "advertisement" in accordance with 18 USC section 1734.

Because the Fe-S cluster of ferrochelatase does not participate directly in catalysis, alternative roles have been proposed (reviewed by Dailey et al[18]). Initial demonstration of decreased ferrochelatase activity in cultured rat hepatocytes treated with S-nitroso-N-acetylpenicillamine,[19] a nitric oxide (NO)-generating compound, prompted 2 further studies, which showed that the cluster is sensitive to destruction by NO in vitro,[20] and in cultured cells.[21] Ferrochelatase activity was also decreased in iron-deprived Cos7 cells expressing human ferrochelatase, but not in cells expressing the non–cluster-containing *E coli* ferrochelatase,[22] suggesting that the cluster may participate in the iron-mediated regulation of human ferrochelatase.[22]

To better understand the role of the Fe-S cluster of ferrochelatase during heme biosynthesis under iron-deficient conditions, we investigated ferrochelatase expression in the iron-deficient erythropoietic tissues of *Irp2*$^{-/-}$ mice, in iron-deprived murine erythroleukemia (MEL) cells, and in human patients with ISCU myopathy.[23,24] Our results demonstrate significant posttranscriptional changes in ferrochelatase expression in *Irp2*$^{-/-}$ splenic erythroblasts. We also found that newly formed, but not mature, ferrochelatase was affected by iron deficiency in MEL cells and that ferrochelatase was dramatically reduced in skeletal muscle of patients with impaired Fe-S cluster assembly because of ISCU depletion. Together, these results demonstrate the potential for modulation of heme biosynthesis via the availability of newly formed Fe-S clusters for insertion into the ferrochelatase apoprotein.

Methods

Animals and cell lines

Irp2$^{-/-}$ and *Irp2*$^{-/-}$*:Irp1*$^{+/-}$ animals were generated as described previously[6] and were more than 1 year of age at the time of analysis. The animals were deeply anesthetized by injection of an isotonic pentobarbital solution containing sodium heparin, and tissues were exsanguinated by cardiac perfusion with phosphate-buffered saline (PBS). Bone marrow was obtained as described previously.[6] All procedures were approved by the National Institute of Child Health and Human Development Animal Care and Use Committee. MEL cells (a gift from Dr David Bodine) were propagated in N-2-hydroxyethylpiperazine-N′-2-ethanesulfonic acid-buffered RPMI 1640 medium (Invitrogen) containing 10% fetal bovine serum at 37°C and 5% CO_2. To induce differentiation, cells were cultured in the presence of 2% dimethyl sulfoxide (DMSO). Under these conditions, the cells cease to divide within 24 hours, and hemoglobin accumulation is evident after 48 hours. All reagents were purchased from Sigma-Aldrich unless otherwise noted.

Splenic erythroblast isolation

Splenic cell suspensions were obtained after perfusion with PBS. Incisions in the capsular membrane were made, and the tissue was rubbed between the frosted portion of 2 microscope slides in PBS. This suspension was passed through a 70-μm strainer, and the filtrate was layered onto Ficoll-Paque PLUS solution (GE Healthcare). Nucleated cells were separated from mature erythrocytes by centrifuging at 1000*g* for 20 minutes at room temperature. The recovered supernatant was washed with Hanks Balanced Salt Solution, and erythroblasts were isolated by incubation with streptavidin-coated Dynabeads (Invitrogen) conjugated to biotinylated anti-TER119 antibody[25] (eBioscience) using the indirect technique according to the manufacturer's instructions. Human Fc fragment (Jackson ImmunoResearch Laboratories) was included to block Fc receptor-mediated binding of nonerythroid cells.

Ferrochelatase assay

Ferrochelatase activity was assayed using modifications to the methods of Shepherd et al,[26] Jones and Jones,[27] and Li et al.[28] Samples were sonicated on ice in lysis buffer consisting of 1% sodium cholate dissolved in 50mM Tris-HCl, pH 8.0. After centrifugation at 20 000*g* for 10 minutes, the supernatants were adjusted to the same total protein concentration after bicinchoninic acid protein assay (Pierce). Ferrochelatase assay buffer consisted of 20mM Tris-HCl (pH 8), 1% Triton X-100, 1mM lauric acid, 50μM deuteroporphyrin IX (Frontier Scientific), and 50μM Zn(II) acetate. A 200- to 400-μg protein sample was added to a UV microcuvette, followed by 10 × assay buffer mixture (without deuteroporphyrin IX) for a final concentration of 1 × assay buffer in 350 μL. Reactions were started by the addition of deuteroporphyrin IX, and the cuvette was placed at 37°C in an Agilent 8453 spectrophotometer. With the UV lamp turned off, visible absorbance spectra were taken in 30-second intervals. Time points between 5 and 10 minutes were used to plot linear kinetic curves. The absorption maximum of the evolving β band (indicative of metal chelation[29]) present in the range of the Q bands at 541 nm was subtracted from an isobestic point of 524 nm present between Q bands IV and III of the unmetallated porphyrin to yield a first-order kinetic rate. For reaction blanks, 2μM N-methyl-mesoporphyrin IX (Frontier Scientific) was included in the reaction mixture of a duplicate sample, which resulted in complete inhibition of the absorbance increase over time. Data are presented as first-order rates, normalized to control samples as either fold-change or percent of control.

Hemoglobin assay

MEL cell hemoglobin levels were assessed semiquantitatively by native polyacrylamide gel electrophoresis (PAGE) separation and electroblotting followed by chromophore-enhanced visualization. Briefly, cell pellets were sonicated in Tris-buffered saline (pH 7.5) and centrifuged for 10 minutes at 20 000*g*, after which the supernatants were centrifuged for 15 minutes at 105 000*g*. The resulting supernatants were adjusted to equivalent protein concentrations, mixed 1:1 with sample buffer (pH 7.5, 100mM Tris-HCl, 15% glycerol, 0.05% bromphenol blue), and 20 to 40 μg of protein was subjected to electrophoresis at 125 V using a 4% to 20% Tris-glycine gel (running buffer was 12mM Tris base, 96mM glycine) until the dye front traveled halfway to the bottom of the gel. Proteins in the gel were electroblotted onto a 0.2-μm pore-size polyvinylidene difluoride filter (Invitrogen) for 1 hour in alcohol-free transfer buffer (25mM Tris base, 192mM glycine) in a Hoefer TE22 transfer apparatus at a current of 400mA and temperature fixed at 20°C. Hemoglobin visualization was enhanced by incubating the filter in a solution of freshly made and filtered 50mM Tris (pH 7.5), 50mM imidazole, 0.5 mg/mL diaminobenzidine, and 0.1% H_2O_2 for 20 minutes in the dark, followed by 2 rinses in water, and 10-minute incubation in a solution consisting of 0.5% (wt/vol) $CuSO_4$ made fresh in 50mM Tris-HCl, pH 7.5. The filter was washed, dried overnight in the dark, and digitized the next morning. Mouse erythrocyte lysate was used as a positive control for hemoglobin in initial experiments. A prominent protein band observed after further staining of the filters with 0.1% Ponceau-S was used as a protein loading control.

Western blots

Sodium dodecyl sulfate (SDS)-PAGE and Western blotting were performed as described previously[30] using 1.5-mm 10% precast bis-Tris gels (Invitrogen), except for ISCU, which was resolved using large-format 15% Tris-glycine gels. Rabbit polyclonal antiferrochelatase serum was a kind gift from Dr Harry Dailey. Mouse monoclonal anti-superoxide dismutase 2 (SOD2) was from Abcam. Antimitochondrial aconitase and ISCU rabbit polyclonal sera were raised against synthetic peptide fragments. Mouse monoclonal anti-protoporphyrinogen oxidase (PPOX) was from Abnova. ALAS2 antibody[6] was affinity purified using a modified surface affinity purification technique. The ALAS2 band, which runs at an aberrantly low apparent molecular weight in bis-Tris gels, was confirmed to be of the correct molecular weight when run in Tris-glycine gels.

Northern blots and quantitative RT-PCR analysis

RNA was extracted using Trizol (Invitrogen) and further purified using the RNeasy kit (QIAGEN) cleanup protocol. Northern blots were performed as reported previously.[6] dsDNA probes were made using α-^{32}P-deoxycytosine triphosphate (PerkinElmer) and the Megaprime labeling kit (GE Healthcare). Probe templates were generated by PCR using a MEL cell cDNA library. Primers were as follows: Probe for both mouse and human ferrochelatase: 5′-ATGGAGAGAGATGGACTAGAGAGGGCC-3′ and 5′-CGCTCTTCTGATGTTCTCAGCTCCACA-3′; mouse β-globin: 5′-GTTGTGTTGACTTGCAACCTCAGA-3′ and 5′-CATTTCCCCACAATTGACAGTTTT-3′. For ALAS2, a probe template was obtained by restriction digestion of a pHIS-Parallel plasmid containing mouse ALAS2 protein coding sequence. Quantitative RT-PCR was performed using SYBR Green (Applied Biosystems) according to the manufacturer's instructions, after reverse transcription of total RNA into cDNA (Applied Biosystems). Quantitative RT-PCR primers were as follows: mouse ferrochelatase 2.2 + 2.9-kb transcripts: 5′-CCTCATCCAGTGCTTTGCAGA-3′ and 5′-GCAGGGAGTGGGCAGAAAAC-3′; mouse ferrochelatase 2.9-kb transcript only: 5′-CGCCTTCATTTGAGTCCACAGT-3′ and 5′-GGCACTGGAAGGTTCCTTGG-3′. Relative transcript abundance was calculated using the $2^{-\Delta\Delta Ct}$ method,[31] with GAPDH as the internal control. Correct quantitative RT-PCR product size was verified by agarose gel electrophoresis.

Aconitase in-gel assay and electrophoretic mobility shift assay

Aconitase was assayed using a coupled assay after native PAGE separation, as described previously.[32] IRP-IRE binding activity was determined by electrophoretic mobility shift assay using a ^{32}P-labeled ferritin IRE probe, as described previously.[32]

Metabolic labeling and pulse-chase

The core protocol for metabolic labeling of MEL cells used in this study is as follows. Cells were washed once in labeling medium (RPMI 1640 without L-cysteine and L-methionine) and incubated in labeling medium for 1 hour, followed by metabolic labeling with the EXPRESS ^{35}S-cysteine and ^{35}S-methionine reagent (1175 Ci/mmol; PerkinElmer) for 10 to 60 minutes. Subsequently, cells were washed with complete RPMI medium and frozen immediately, or washed twice and chased in treatment medium for various time points. Cell pellets were lysed in Tris-buffered saline with 1% Triton X-100, centrifuged at 20 000*g* for 10 minutes, and adjusted to equal total protein concentration. Immunoprecipitation was carried out essentially as described previously,[33] with 750 μg of total protein and 1.5 μL of ferrochelatase antiserum used per sample. Wash and binding buffer consisted of 1% NP-40 and 0.5% deoxycholate in PBS. Immunoprecipitated radiolabeled ferrochelatase was visualized by SDS-PAGE in 10% bis-Tris gels with MOPS-SDS running buffer (Invitrogen), followed by autoradiography with Kodak MR single emulsion films.

Tissue biopsies and myoblast cultures

Control and ISCU myopathy patient skeletal muscle was obtained and prepared as described previously.[23] Written consent was given by all persons involved in the study in accordance with the Institutional Review Board for Human Studies of the University of Texas, Southwestern Medical School, and the Declaration of Helsinki. Primary myoblast cell lines, a generous gift from Dr Eric Shoubridge, were cultured on BD Matrigel-coated flasks as described previously,[34] except that Lonza SKBM-2 culture medium was used. Terminal differentiation of myoblasts into myotubes was achieved by incubation of the cultures for 4 days in Dulbecco modified Eagle medium containing 2% heat-inactivated horse serum (Invitrogen).

Results

Posttranscriptional alteration of ferrochelatase expression in iron-deficient erythropoietic tissues of *Irp2*$^{-/-}$ mice

Depleted cellular iron stores and microcytic anemia have been correlated with reduced TfR1 protein expression levels in the developing erythroblasts of *Irp2*$^{-/-}$ mice.[6] To investigate the expression of ferrochelatase in functionally iron-deficient erythroid tissue, ferrochelatase activity, protein, and mRNA levels were measured in bone marrow and spleens of wild-type (*Irp1*$^{+/+}$:*Irp2*$^{+/+}$) and *Irp2*$^{-/-}$ (*Irp1*$^{+/+}$:*Irp2*$^{-/-}$) mice. Ferrochelatase activity, protein levels, and mRNA abundance were all decreased in *Irp2*$^{-/-}$ bone marrow aspirates compared with wild-type animals (Figure 1A-C); however, whereas ferrochelatase activity and protein levels were also decreased in *Irp2*$^{-/-}$ spleens (Figure 1D-E), ferrochelatase mRNA levels were increased (Figure 1F). Northern blots of β-globin in bone marrow aspirates demonstrated decreased β-globin mRNA levels in *Irp2*$^{-/-}$ mice and in *Irp2*$^{-/-}$ mice lacking one allele of *Irp1* (*Irp1*$^{+/-}$:*Irp2*$^{-/-}$; Figure 1G), whereas spleen β-globin mRNA levels were elevated in *Irp2*$^{-/-}$ and *Irp1*$^{+/-}$:*Irp2*$^{-/-}$ mice (Figure 1H). Splenic expression levels of the erythroid-specific transcription factors *Gata1* and *Hmgb3* were also increased, as measured by quantitative RT-PCR (data not shown). These data suggest that erythropoietic activity shifted somewhat from the bone marrow to the spleen in *Irp2*$^{-/-}$ and *Irp1*$^{+/-}$:*Irp2*$^{-/-}$ animals, which might explain the changes in ferrochelatase mRNA levels observed in bone marrow and spleens of *Irp2*$^{-/-}$ mice.

To eliminate the effect of differences in splenic cellularity on our analysis of ferrochelatase expression, TER119^{+} erythroid cells were isolated from animals of the 3 genotypes, and ferrochelatase mRNA and protein levels in each sample were evaluated by quantitative RT-PCR and Western blot. Ferrochelatase protein was significantly decreased in splenic TER119^{+} erythroid cells from *Irp2*$^{-/-}$ and *Irp1*$^{+/-}$:*Irp2*$^{-/-}$ animals (Figure 1I); and despite some variation in protein and mRNA levels, the calculated protein/mRNA ratio was significantly decreased in the *Irp2*$^{-/-}$ and *Irp1*$^{+/-}$:*Irp2*$^{-/-}$ samples (Figure 1J). Notably, mild decreases in ferrochelatase activity and protein levels were also observed in the kidneys and livers of *Irp1*$^{+/-}$:*Irp2*$^{-/-}$ mice in the absence of measurable changes in ferrochelatase mRNA levels, whereas ferrochelatase activity and protein levels were unchanged in whole brain and heart extracts (data not shown).

Posttranscriptional regulation of ferrochelatase in MEL cells during iron depletion and oxidative stress

To allow for further investigation of the posttranscriptional regulation of ferrochelatase in developing erythroid cells, we established a model of iron-limited erythroid differentiation using MEL cells. Treatment of MEL cells with 2% DMSO induces rapid progression of MEL cells from a stage resembling late erythroid colony-forming units to a stage resembling basophilic and orthochromatophilic erythroblasts in the erythroid lineage,[35] where globin expression and hemoglobin formation are observed, along with increased expression of ferrochelatase mRNA and protein.[36] Treatment of differentiating MEL cells concomitantly with the iron chelator desferrioxamine (DFO) caused a sustained increase in IRE binding activity of IRP1 and IRP2 (Figure 2B), whereas the differentiation-induced increase in activity of the [4Fe-4S] cluster-containing mitochondrial and cytosolic aconitases was attenuated (Figure 2C), consistent with cellular iron depletion. Induction of *Alas2* mRNA expression was observed during differentiation of MEL cells under both normal and iron-depleted conditions (Figure 2D). However, ALAS2 protein levels remained repressed in iron-deficient MEL cells (Figure 2E), presumably because of increased IRP-mediated translational repression. Finally, hemoglobin formation was attenuated in iron-depleted MEL cells (Figure 2F), an effect that was

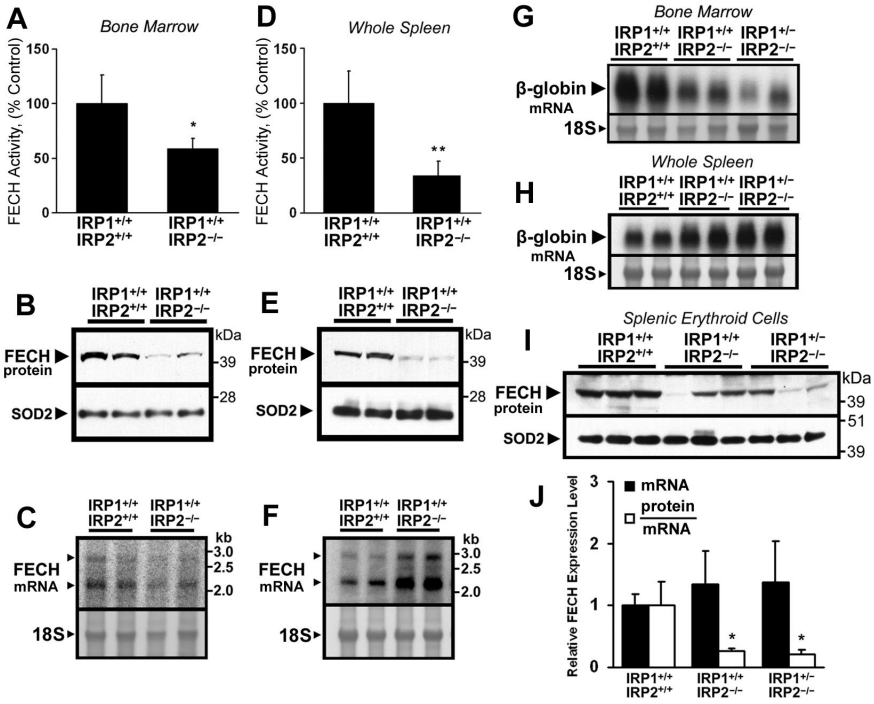

Figure 1. Posttranscriptional reduction of ferrochelatase (FECH) activity and protein levels in erythropoietic tissues of *IRP2*$^{-/-}$ mice. (A,D) FECH activity in bone marrow aspirates and whole spleens of *Irp1*$^{+/+}$:*Irp2*$^{-/-}$ mice was significantly decreased compared with *Irp1*$^{+/+}$:*Irp2*$^{+/+}$ (wild-type) animals. Error bars represent SD (n = 4 animals per genotype). (B,E) FECH protein levels in bone marrow and spleen were also decreased in *Irp1*$^{+/+}$:*Irp2*$^{-/-}$ animals. Each lane from the Western blot represents whole-tissue protein extracts pooled from 2 animals. The filter was reprobed for SOD2 as a loading control for mitochondrial matrix protein. (C,F) FECH mRNA levels were increased in the spleens of *Irp1*$^{+/+}$:*Irp2*$^{-/-}$ mice. Messenger RNA levels were measured by Northern blot using a probe specific for both the 2.2-kb and 2.9-kb FECH transcripts; each lane represents RNA pooled equally from 2 animals. The 18S ribosomal band was visualized to assess equal loading. Results were confirmed by quantitative RT-PCR (data not shown). (G-H) To estimate the tissue distribution of erythroid cells, β-globin mRNA levels in bone marrow aspirates and spleens from *Irp1*$^{+/+}$: *Irp2*$^{+/+}$, *Irp1*$^{+/+}$:*Irp2*$^{-/-}$, and *Irp1*$^{+/-}$:*Irp2*$^{-/-}$ mice were assessed by Northern blot. (I) FECH protein abundance in splenic TER119^{+} erythroid cells mice was measured by Western blot. FECH mRNA transcript levels (J, ■) were measured by quantitative RT-PCR using primers specific for both the 2.2-kb and 2.9-kb FECH transcripts; data are normalized to *Irp1*$^{+/+}$:*Irp2*$^{+/+}$ (wild-type) mRNA levels. Relative protein abundance was calculated by densitometry, and individual protein abundance values were normalized to the respective mRNA levels measured in the same sample (J, □). Data in panels A, D, and J were analyzed by 2-tailed Student *t* test; *$P < .05$; **$P < .01$.

probably the result of a combination of decreased iron availability and repressed ALAS2 protein induction.[37]

As reported previously,[36] expression of both the short (2.2-kb) and long (2.9-kb) isoforms of ferrochelatase mRNA transcripts increased during DMSO-induced differentiation of MEL cells (Figure 3A), leading to increased ferrochelatase activity and protein levels (Figure 3A-B). In contrast, ferrochelatase activity and protein levels were attenuated in iron-depleted differentiating MEL cells, despite comparable increases in ferrochelatase mRNA (Figure 3C-D). In summary, differentiation of MEL cells under iron-deficient conditions faithfully reproduces the posttranscriptional decrease of ferrochelatase protein observed in iron-deficient *Irp2*$^{-/-}$ erythroblasts shown in Figure 1, and as reported previously in DFO-treated K562 cells,[22] providing us with a system to further evaluate how ferrochelatase protein and activity decrease during iron deficiency.

In contrast to the effects of iron depletion, we observed greater abundance and activity of ferrochelatase in MEL cells cultured in a 6% O_2 versus a 21% O_2 atmosphere for several days, followed by induction of differentiation by treatment with DMSO (Figure 4B-C). As ferrochelatase mRNA levels were not increased in cells grown in 6% O_2 compared with cells grown at 21% O_2 (Figure 4D), we surmise that the ferrochelatase holo-protein is stabilized under reduced cellular oxygen concentrations in vivo, consistent with the original report of reduced stability of the purified enzyme under aerobic conditions in vitro.[13] The increased ferrochelatase activity and protein levels in cells cultured at 6% O_2 were associated with increased ALAS2 protein expression (Figure 4E) and enhanced hemoglobin production (Figure 4F), demonstrating that hemoglobinization of MEL cells is more rapid at reduced oxygen levels. To further investigate the sensitivity of ferrochelatase to oxidative damage in vivo, we treated MEL cells with the redox-cycling mitochondrial pro-oxidant menadione.[38] Brief treatment of MEL cells with a range of menadione concentrations resulted in a rapid dose-dependent depletion of total cellular ferrochelatase protein levels within 3 hours (Figure 4G), whereas the abundance of several other mitochondrial enzymes, including PPOX, mitochondrial aconitase (mACO), and SOD2 was not affected within this time period. These data suggest that mature Fe-S cluster-containing ferrochelatase is rapidly degraded during conditions of mitochondrial oxidative stress.

Stability of newly formed, but not mature, ferrochelatase depends on iron availability

To better understand the mechanism by which depletion of cellular iron leads to decreased levels of ferrochelatase protein, we performed a series of metabolic labeling experiments to assess the fate of ferrochelatase in MEL cells under the iron-limited differentiation conditions used in Figure 3. In the first experiment, the cells were labeled with ^{35}S-cysteine and ^{35}S-methionine for a brief (10-minute) period after a 24-hour treatment of differentiating MEL cells with DFO. These conditions were used to estimate the "instantaneous" synthesis rate of the ferrochelatase apoprotein under iron-limited conditions. Although total cellular ferrochelatase levels were reproducibly reduced in iron-depleted cells, the

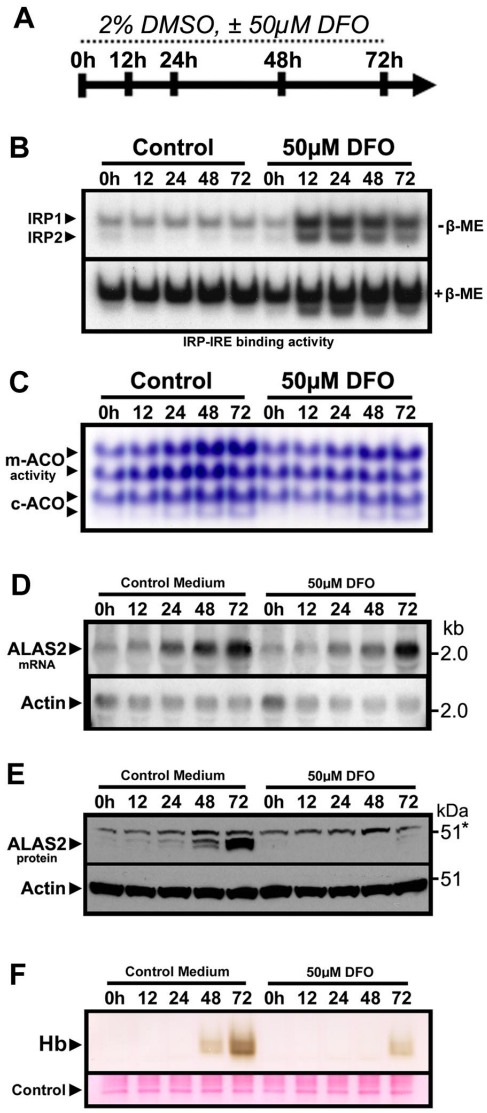

Figure 2. Iron-limited erythroid differentiation of MEL cells. (A) Timeline depicting the experimental time course of DMSO-induced erythroid differentiation of MEL cells under normal conditions or iron-deficient conditions induced by the iron chelator DFO. (B) Electrophoretic mobility shift assay of MEL cell protein extracts using a ^{32}P-labeled ferritin IRE probe showed activation of IRP1 and IRP2 after treatment with DFO. (C) Aconitase activity gel demonstrating a time-dependent increase in mitochondrial (m-) and cytosolic (c-) aconitase activity levels over the course of differentiation, which was attenuated in DFO-treated cultures. (D) ALAS2 mRNA was induced during differentiation in the presence or absence of DFO. However, ALAS2 protein expression (E) was repressed in DFO-treated cells. Sample loading was assessed by reprobing for actin mRNA and protein, respectively. (F) Mature (heme-containing) hemoglobin (Hb) formation was repressed in differentiating MEL cells treated with DFO. Hemoglobin was measured by a modified diaminobenzidine procedure after separation of total cellular protein (40 μg) by native PAGE followed by transfer to polyvinylidene difluoride filters ("Hemoglobin assay").

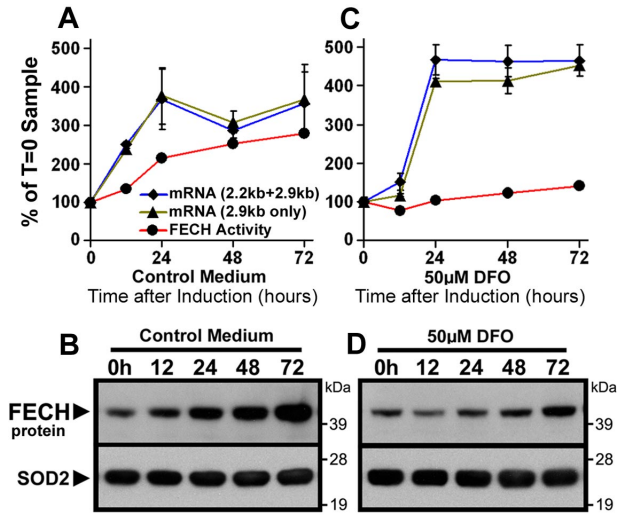

Figure 3. Posttranscriptional reduction of FECH in MEL cells during iron-limited differentiation. (A,C) Induction of FECH enzyme activity (red line), but not mRNA levels (blue, green lines), was repressed during differentiation in the presence of DFO. FECH mRNA levels were measured by quantitative RT-PCR as described in "Northern blots and quantitative RT-PCR analysis." mRNA transcript and enzyme activity levels are normalized to T = 0 samples. (B,D) Induction of FECH protein levels during differentiation was attenuated in cells cotreated with DFO, despite increased FECH mRNA levels. FECH protein levels were measured by Western blot, and the filter was reprobed for SOD2 as a loading control for mitochondrial matrix proteins.

rate of synthesis of newly labeled ferrochelatase polypeptides in iron-depleted cells during the 10-minute labeling period was not different from control cells (Figure 5A).

In the subsequent experiment, MEL cells were metabolically labeled for 1 hour and were then incubated in normal medium for 3 hours to allow for the newly labeled ferrochelatase proteins to completely fold and obtain Fe-S clusters before the onset of iron deficiency. Subsequently, the cells were treated with DMSO plus or minus DFO for 24 hours, and were then harvested and analyzed for total and radiolabeled ferrochelatase as in the previous experiment. Results of this experiment (Figure 5B) demonstrate that the ferrochelatase polypeptides that were allowed to mature fully before the onset of iron deficiency were not susceptible to degradation, although total cellular ferrochelatase levels were again diminished in the DFO-treated cells.

In the final experiment, MEL cells were first treated with DMSO plus or minus DFO for 24 hours, followed by metabolic labeling for 40 minutes. Subsequently, the cells were incubated in normal medium for various periods of time followed by assessment of the remaining radiolabeled ferrochelatase (Figure 5C). We found that the half-life of newly formed ferrochelatase was dramatically reduced in the iron-depleted cells (Figure 5C-D), in which newly formed ferrochelatase polypeptides had a calculated half-life of less than 1 hour. In contrast, ferrochelatase showed a calculated half-life of approximately 35 hours in control cells. Together, these data suggest that newly formed ferrochelatase protein that has not fully folded into the mature form within the mitochondrion is highly susceptible to degradation under iron-deficient conditions.

Disruption of Fe-S cluster assembly results in diminished cellular ferrochelatase levels

The data in Figure 5 suggested that impairment of mitochondrial Fe-S cluster assembly by iron depletion could result in enhanced degradation of newly formed ferrochelatase polypeptides by limiting the availability of free [2Fe-2S] clusters for insertion into the apoprotein. To test the dependence of ferrochelatase stability on availability of newly formed Fe-S clusters, we measured ferrochelatase levels in muscle biopsies and cultured myoblasts from patients with ISCU myopathy, a disease characterized by impaired Fe-S cluster assembly in muscle tissue resulting from deficiency of the Fe-S cluster scaffold protein ISCU[23,24] (Figure 6A). Ferrochelatase protein levels were dramatically depleted in ISCU patient muscle biopsies, compared with 3 control biopsies and one biopsy obtained from a patient with an unrelated mitochondrial myopathy (Figure 6B). As shown previously,[23] levels of [4Fe-4S]-containing mACO were also depleted in the ISCU myopathy patients (Figure 6B).

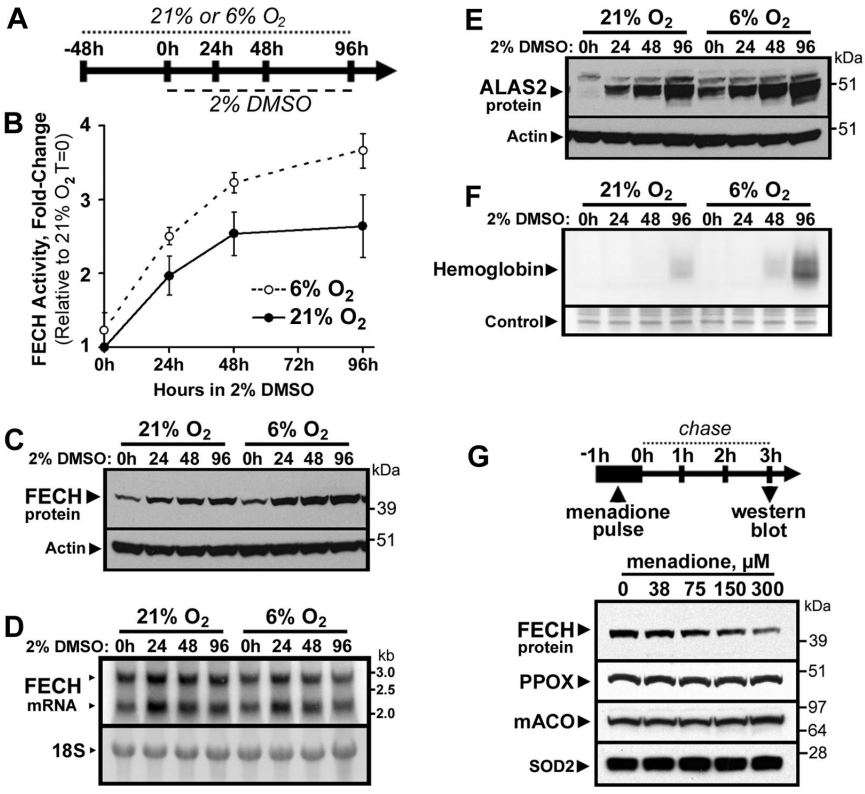

Figure 4. FECH is destabilized by oxygen and mitochondrial oxidative stress. (A) Cells were maintained in normal (21%) or reduced (6%) O_2 atmosphere, followed by differentiation by DMSO treatment. FECH activity (B) and protein levels (C) were increased in differentiating MEL cells maintained at 6% O_2 relative to 21% O_2 cultures. However, FECH mRNA levels (D) in 6% O_2 cultures were not greater than those in 21% O_2 cultures. (E) ALAS2 protein expression was also elevated in cells cultured in 6% O_2 relative to 21% O_2 cultures. (F) Hemoglobinization was accelerated in differentiating cells cultured in 6% O_2 (20 μg of total protein was loaded). (G) Menadione-induced mitochondrial oxidative stress caused rapid and specific depletion of total cellular FECH protein levels, whereas PPOX, mACO, and SOD2 protein levels were not appreciably altered. Error bars in panel B represent the range of 2 experimental replicates.

To further investigate ferrochelatase expression levels during ISCU depletion, a differentiation time-course experiment was performed using cultured myotubes isolated from an ISCU myopathy patient and control myotubes isolated from a normal person. Both ISCU and ferrochelatase protein levels increased significantly during the course of differentiation of the myoblasts into myotubes (Figure 6C). However, marked ISCU depletion was observed in the patient cultures, which was accompanied by decreased ferrochelatase protein levels relative to the control at every respective time point (Figure 6C). In contrast, ferrochelatase mRNA levels, measured in control and patient myotube cultures at 0 and 5 days of differentiation by Northern blot (Figure 6D) and quantitative PCR (data not shown), did not reflect the dramatic decrease in ferrochelatase protein levels observed in the patient tissues (Figure 6B) and

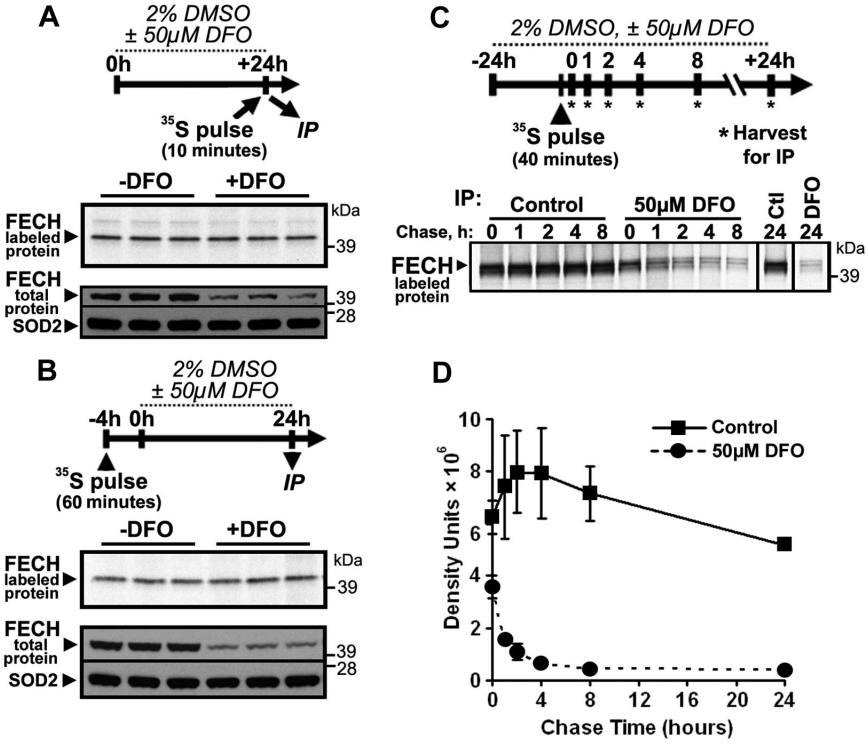

Figure 5. Newly formed, but not mature, FECH protein is susceptible to regulation by iron availability. (A) To test for changes in the instantaneous synthesis rate of FECH protein under iron-depleted conditions, MEL cells were differentiated for 24 hours in the presence or absence of DFO, and harvested immediately after a rapid 10-minute pulse with ^{35}S-Cys and ^{35}S-Met. Radiolabeled FECH was visualized by autoradiography after immunoprecipitation and SDS-PAGE (top panel), whereas total protein levels were measured by Western blot (bottom panel). (B) The effect of iron limitation on mature, Fe-S cluster-containing FECH was assessed by metabolic labeling of cells for 1 hour with ^{35}S-Cys and ^{35}S-Met 4 hours before the onset of 24 hours of differentiation and DFO treatment. After 24-hour incubation, cells were harvested and analyzed for radiolabeled and total protein levels as in panel A. (C) A pulse-chase experiment was performed to follow the fate of newly formed FECH protein during normal and iron-limited growth conditions. After 24-hour differentiation in the presence or absence of DFO, cells were pulsed for 40 minutes with ^{35}S-Cys and ^{35}S-Met, followed by incubation for various periods of time in differentiation medium with or without DFO. A representative autoradiogram is shown; the results of 2 experiments are quantified and plotted in panel D.

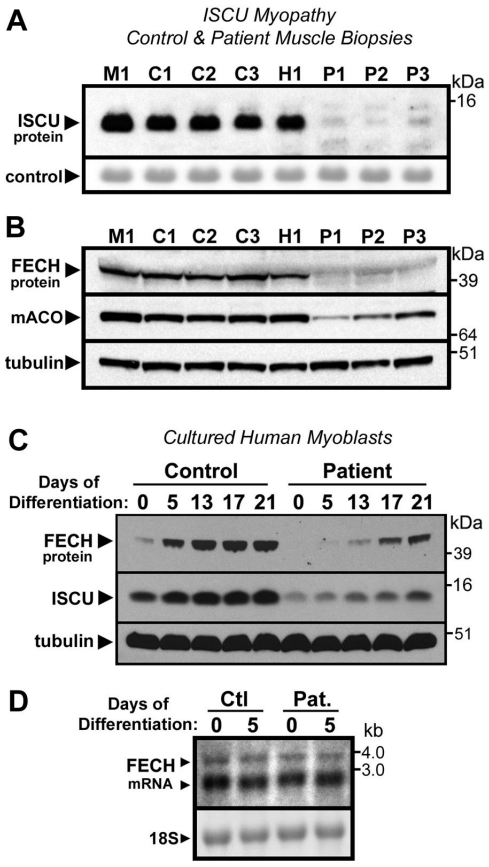

Figure 6. Disruption of Fe-S assembly in ISCU myopathy causes depletion of FECH. (A) As reported previously, total ISCU protein levels were depleted in vastus lateralis muscle biopsies taken from Swedish patients with ISCU myopathy (lanes designated as P1-P3), compared with 3 healthy controls (designated C1-C3), and a patient with an unrelated mitochondrial myopathy (designated as M1). A prominent protein band observed after Ponceau-S staining of the filter served as the loading control. (B) FECH protein levels were also greatly decreased in the ISCU myopathy biopsies, as were levels of the Fe-S cluster-containing enzyme mitochondrial aconitase. (C) Primary myotube cultures obtained from an ISCU myopathy patient as well as from a healthy person (control) were terminally differentiated by growth in low serum conditions ("Tissue biopsies and myoblast culture"). Although FECH and ISCU levels increased in both control and patient cultures during the course of the experiment, the relative level of both proteins was diminished in the patient cultures compared with the control at every given time point. (D) Little difference in FECH mRNA levels was seen in control and patient myotube cultures at zero and 5 days of differentiation, as assessed by Northern blot.

myotube cultures (Figure 6C), confirming posttranscriptional regulation of ferrochelatase during conditions of impaired Fe-S cluster assembly in the ISCU myopathy patients.

Discussion

Since the significant discovery that mammalian ferrochelatase is an Fe-S cluster-containing protein,[13] there has been continued speculation on possible biologic functions of the cluster, which has been renewed after biochemical and structural reports demonstrating that the cluster does not participate directly in enzymatic catalysis.[12,14] In this study, we report significant posttranscriptional depletion of ferrochelatase during iron-deficient erythropoiesis in *Irp2*$^{-/-}$ mouse erythroid tissue, during iron-limited erythroid differentiation of MEL cells in vitro, and during conditions of impaired de novo Fe-S cluster assembly in human patients affected by ISCU myopathy. Together, these findings suggest that ferrochelatase expression is significantly influenced by the availability of newly formed Fe-S clusters, the biogenesis of which is reliant on the continued availability of iron as well as functional Fe-S cluster assembly machinery. Recently, a pool of genes that coexpress with the heme biosynthetic enzymes was reported,[39] and several of these genes have been implicated (*C1orf69*[40]) or are known to participate directly (*GLRX5*,[41] *ISCA1* and *ISCA2*[42]) in Fe-S cluster assembly. These observations, along with the results presented here, provide further evidence for an inextricable link between Fe-S cluster assembly and heme biosynthesis.

Decreased ferrochelatase expression during iron-limited erythropoiesis in *Irp2*$^{-/-}$ mice

Ferrochelatase is essential for heme biosynthesis in all mammalian cells, and ferrochelatase expression is robustly up-regulated in developing erythroid cells by transcriptional activation via a single promoter containing Sp1, NF-E2, and GATA elements.[43] In erythroid cells, iron limitation decreases heme biosynthesis via IRP-mediated translational repression of ALAS2 because of the presence of an IRE in its 5′-UTR,[4] and loss of this repression in *Irp2*$^{-/-}$ mice undoubtedly contributes to the more than 100-fold increase in PPIX observed within their erythrocytes.[6] Here we report an additional alteration in the heme biosynthetic pathway in *Irp2*$^{-/-}$ mice, namely, posttranscriptional depletion of ferrochelatase protein levels in developing *Irp2*$^{-/-}$ splenic erythroblasts. Despite the significantly increased levels of ferrochelatase, β-globin, and other erythroid-specific mRNA transcripts observed in *Irp2*$^{-/-}$ spleens, probably a consequence of enhanced extramedullary hematopoiesis, ferrochelatase activity and protein levels were significantly decreased (Figure 1). Erythropoietic cells in *Irp2*$^{-/-}$ mice are considered to be constitutively iron-deficient because of multiple factors, including decreased expression of TfR1.[6,7] We hypothesize that iron deficiency within developing *Irp2*$^{-/-}$ erythroblasts limits the availability of newly formed Fe-S clusters for insertion into ferrochelatase apoproteins. Further, we predict that the ferrochelatase apoprotein is rapidly degraded by mitochondrial proteases when it cannot obtain an Fe-S cluster because the cluster-ligating carboxy-terminal region of the protein is important for folding and dimerization of the mature enzyme,[12,16] and mutations in this region result in EPP in humans.[17]

Posttranslational decrease in ferrochelatase protein during iron-limited erythropoiesis and oxidative stress in MEL cells

To more closely examine the fate of ferrochelatase during cellular iron deficiency, we used differentiating MEL cells grown under mildly iron-deficient conditions, characterized by activation of IRPs, repression of ALAS2 protein expression, and delayed hemoglobin formation. The expected increase in ferrochelatase protein levels during differentiation was strongly attenuated under these conditions, even though ferrochelatase mRNA levels were elevated. Cellular iron deficiency might alter ferrochelatase levels by repressing the translation of ferrochelatase polypeptides, by reducing the de novo formation of mature culster-containing holo-protein, or by decreasing the stability of the mature holoprotein. Using metabolic labeling and pulse-chase experiments, we found no alteration in the instantaneous synthesis rate of ferrochelatase during iron deficiency; however, the apparent half-life of the newly formed ferrochelatase was dramatically reduced from approximately 35 hours in normal cells to less than 1 hour in iron-deficient cells. Perhaps most importantly, no change in the abundance of ^{35}S-labeled mature ferrochelatase protein was observed after iron depletion. Together, we interpret these results to

suggest that mature mitochondrial [2Fe-2S] cluster-containing holo-ferrochelatase is not susceptible to degradation during iron deficiency, whereas newly formed apo-ferrochelatase is rapidly degraded in the absence of available iron.

In contrast to cellular iron deficiency, where we observed no depletion of mature ferrochelatase, we did observe very rapid (within 3 hours) decreases in total cellular ferrochelatase levels after menadione treatment, which cannot be explained by impaired maturation of the apoprotein because of the short timeframe of the experiment. Together with our finding of increased ferrochelatase stability in MEL cells grown at reduced O_2 levels, these data suggest that the oxidative modification of mature ferrochelatase, probably involving alteration or destruction of the Fe-S cluster, leads to rapid degradation of the protein. These results are consistent with the previous report on decreased stability of ferrochelatase under aerobic conditions in vitro,[13] and other reports concerning the sensitivity of ferrochelatase to nitric oxide.[19-21]

Ferrochelatase protein expression depends on Fe-S cluster availability

It is logical to predict that the diminished maturation of ferrochelatase polypeptides in the mitochondria of iron-depleted cells is the result of impaired de novo formation of [2Fe-2S] clusters by the mitochondrial Fe-S cluster assembly machinery because of lack of available iron ions. Under this prediction, one would expect a similar decrease in cellular ferrochelatase levels after impairment of the Fe-S assembly machinery by means other than iron depletion. To test this hypothesis, we measured cellular ferrochelatase levels in muscle biopsies and cultured myoblasts obtained from Swedish patients with ISCU myopathy, a mitochondrial myopathy with exercise intolerance that was recently shown to be a result of deficiency of the Fe-S cluster scaffold protein ISCU.[23,24] In these patients, the activity and abundance of several Fe-S-containing proteins, including aconitase and succinate dehydrogenase, are greatly reduced,[44] leading to impaired muscle oxidative phosphorylation, lactic acidosis, and episodes of acute rhabdomyolysis and myoglobinuria.[44,45]

Here, we report a dramatic reduction in ferrochelatase protein levels in ISCU myopathy patients, demonstrating that impaired Fe-S cluster assembly in the absence of iron depletion also decreases ferrochelatase expression posttranscriptionally. We predict that a similar mechanism can explain our observations during both cellular iron deficiency and during impaired Fe-S cluster assembly. Decreased availability of newly formed Fe-S clusters caused either by a lack of available iron or by impairment of the Fe-S cluster assembly machinery results in impaired maturation of apo-ferrochelatase and subsequent rapid degradation by unknown proteases (Figure 7). In contrast, alteration or destruction of the Fe-S cluster of holo-ferrochelatase during oxidative stress or in the presence of nitric oxide rapidly leads to degradation of the mature pool of ferrochelatase, which is otherwise resistant to iron depletion and impairment of Fe-S cluster assembly. Thus, the capacity for cellular heme biosynthesis could be altered by decreased ferrochelatase protein levels brought on by iron deficiency, defects in Fe-S cluster assembly machinery, or oxidative conditions causing Fe-S cluster degradation.

Our findings of decreased ferrochelatase abundance during impaired Fe-S assembly in ISCU myopathy are consistent with recent findings in the mouse model of Friedreich ataxia.[46] Decreases in the abundance of mitochondrial Fe-S cluster-containing proteins, including ferrochelatase, were observed in cardiac tissue of mice lacking frataxin,[46] the deficiency of which is known to result in impaired Fe-S cluster assembly, accompanied by cerebellar ataxia and cardiomyopathy (reviewed elsewhere[47]). These authors also reported increases in the mitochondrial proteases ClpP and Lon in affected mouse cardiac tissue, suggesting a pathway by which accumulating Fe-S cluster-deficient ferrochelatase and other apoproteins might be degraded.[46] It will be interesting to determine the exact pathway for proteolytic degradation of immature apo-ferrochelatase in the mitochondrion, although this is currently a

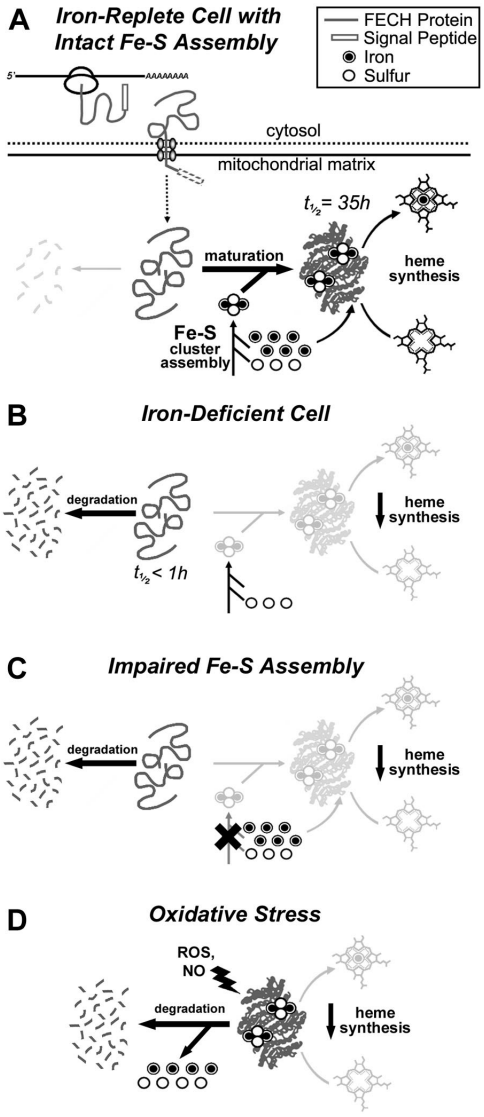

Figure 7. The impact of cellular iron deficiency, impaired Fe-S biosynthesis, and mitochondrial oxidative stress on FECH activity and protein levels. (A) A schematic representation of the synthesis, mitochondrial translocation, and maturation of FECH polypeptides under normal conditions. FECH protein is synthesized on cytosolic ribosomes and translocated into the mitochondrion where its signal peptide is cleaved. Complete folding and maturation of FECH requires the provision of a newly formed Fe-S cluster, which is supplied by the Fe-S cluster assembly machinery. After folding and insertion of the cluster, FECH can catalyze the final step in the heme biosynthetic pathway, which is the insertion of ferrous iron into protoporphyrin IX. (B) Under conditions of cellular iron depletion, de novo Fe-S cluster assembly in the mitochondrion is halted because of the lack of available iron ions, and newly imported apo-FECH accumulates and is rapidly degraded within the mitochondrion. (C) Similarly, if mitochondrial Fe-S assembly is disrupted in the absence of cellular iron depletion, as in ISCU myopathy, apo-FECH fails to obtain Fe-S clusters and is rapidly degraded. (D) Under conditions of mitochondrial oxidative stress, mature Fe-S cluster-containing FECH is rapidly destabilized. Degradation is probably initiated by chemical modification or disassembly of the Fe-S cluster, resulting in a conformational change and degradation of the FECH polypeptide.

difficult question to address because of the lack of specific inhibitors of the mammalian mitochondrial protein degradation machinery.[48]

The deficiency of ferrochelatase in ISCU myopathy might help to explain the decreased cytochrome oxidase (complex IV) activity observed in some ISCU myopathy patients.[49] Indeed, the most dramatic decrease in cytochrome oxidase activity was in 2 brothers with a more severe compound-heterozygotic form of ISCU myopathy.[49] Although cytochrome oxidase does not contain iron-sulfur clusters, it does contain 2 heme cofactors essential for electron transport. We propose that the substantial loss of ferrochelatase resulting from impaired Fe-S cluster assembly in these patients may lead to an inadequate availability of heme for assembly into newly formed apo-hemoproteins, such as cytochrome oxidase. Thus, the loss of ferrochelatase could clearly contribute to the oxidative defects observed in the mitochondrial respiratory chain of these patients.

In conclusion, we have identified several in vivo situations in which robust posttranscriptional decrease in ferrochelatase levels occurs in conjunction with cellular iron deficiency, defective Fe-S cluster assembly, or oxidative stress. Iron deficiency in developing $Irp2^{-/-}$ red cells or in MEL cells leads to decreased maturation of Fe-S cluster-containing ferrochelatase, whereas deficiency in the Fe-S cluster assembly machinery in the muscles of ISCU myopathy patients also leads to substantial depletion of ferrochelatase, perhaps contributing to the pathogenesis of this disease. Together, these results provide concrete examples of an inextricable link between the essential processes of Fe-S cluster assembly and heme biosynthesis.

Acknowledgments

The authors thank Drs Harry Dailey and Manu Hegde for helpful scientific discussions, Dr Eric Shoubridge for providing the primary myoblast cells, and Drs Kuanyu Li, Deliang Zhang, Helge Uhrigshardt, Gennadiy Kovtunovych, and Sharon Cooperman for providing ideas and suggestions that greatly improved the quality of this work.

This work was supported by the National Institute of Child Health and Human Development Intramural Research Program, National Institute of Arthritis and Musculoskeletal and Skin Diseases (R01 AR050597), and a Veterans Affairs Merit Review.

Authorship

Contribution: D.R.C. designed and performed experiments, analyzed data, and prepared the manuscript; M.C.G. performed experiments; R.G.H. provided vital reagents; W.-H.T and T.A.R oversaw the study and designed experiments; and T.A.R. also assisted in manuscript preparation.

Conflict-of-interest disclosure: The authors declare no competing financial interests.

Correspondence: Tracey A. Rouault, Molecular Medicine Program, *Eunice Kennedy Shriver* National Institute of Child Health and Human Development, Bldg 18T, Rm 101, 9000 Rockville Pike, Bethesda, MD 20892; e-mail: trou@helix.nih.gov.

References

1. Kikuchi G, Kumar A, Talmage P, Shemin D. The enzymatic synthesis of delta-aminolevulinic acid. *J Biol Chem.* 1958;233(5):1214-1219.
2. Ajioka RS, Phillips JD, Kushner JP. Biosynthesis of heme in mammals. *Biochim Biophys Acta.* 2006;1763(7):723-736.
3. Nishida G, Labbe RF. Heme biosynthesis; on the incorporation of iron into protoporphyrin. *Biochim Biophys Acta.* 1959;31(2):519-524.
4. Cox TC, Bawden MJ, Martin A, May BK. Human erythroid 5-aminolevulinate synthase: promoter analysis and identification of an iron-responsive element in the mRNA. *EMBO J.* 1991;10(7):1891-1902.
5. Binder R, Horowitz JA, Basilion JP, Koeller DM, Klausner RD, Harford JB. Evidence that the pathway of transferrin receptor mRNA degradation involves an endonucleolytic cleavage within the 3′-UTR and does not involve poly(A) tail shortening. *EMBO J.* 1994;13(8):1969-1980.
6. Cooperman SS, Meyron-Holtz EG, Olivierre-Wilson H, Ghosh MC, McConnell JP, Rouault TA. Microcytic anemia, erythropoietic protoporphyria, and neurodegeneration in mice with targeted deletion of iron-regulatory protein 2. *Blood.* 2005; 106(3):1084-1091.
7. Galy B, Ferring D, Minana B, et al. Altered body iron distribution and microcytosis in mice deficient in iron regulatory protein 2 (IRP2). *Blood.* 2005; 106(7):2580-2589.
8. Bloomer J, Bruzzone C, Zhu L, Scarlett Y, Magness S, Brenner D. Molecular defects in ferrochelatase in patients with protoporphyria requiring liver transplantation. *J Clin Invest.* 1998; 102(1):107-114.
9. Brenner DA, Didier JM, Frasier F, Christensen SR, Evans GA, Dailey HA. A molecular defect in human protoporphyria. *Am J Hum Genet.* 1992; 50(6):1203-1210.
10. Bonkowsky HL, Bloomer JR, Ebert PS, Mahoney MJ. Heme synthetase deficiency in human protoporphyria: demonstration of the defect in liver and cultured skin fibroblasts. *J Clin Invest.* 1975; 56(5):1139-1148.
11. Gouya L, Puy H, Lamoril J, et al. Inheritance in erythropoietic protoporphyria: a common wild-type ferrochelatase allelic variant with low expression accounts for clinical manifestation. *Blood.* 1999;93(6):2105-2110.
12. Wu CK, Dailey HA, Rose JP, Burden A, Sellers VM, Wang BC. The 2.0 A structure of human ferrochelatase, the terminal enzyme of heme biosynthesis. *Nat Struct Biol.* 2001;8(2):156-160.
13. Dailey HA, Finnegan MG, Johnson MK. Human ferrochelatase is an iron-sulfur protein. *Biochemistry.* 1994;33(2):403-407.
14. Medlock AE, Dailey HA. Examination of the activity of carboxyl-terminal chimeric constructs of human and yeast ferrochelatases. *Biochemistry.* 2000;39(25):7461-7467.
15. Sellers VM, Wang KF, Johnson MK, Dailey HA. Evidence that the fourth ligand to the [2Fe-2S] cluster in animal ferrochelatase is a cysteine: characterization of the enzyme from Drosophila melanogaster. *J Biol Chem.* 1998;273(35):22311-22316.
16. Crouse BR, Sellers VM, Finnegan MG, Dailey HA, Johnson MK. Site-directed mutagenesis and spectroscopic characterization of human ferrochelatase: identification of residues coordinating the [2Fe-2S] cluster. *Biochemistry.* 1996;35(50): 16222-16229.
17. Schneider-Yin X, Gouya L, Dorsey M, Rufenacht U, Deybach JC, Ferreira GC. Mutations in the iron-sulfur cluster ligands of the human ferrochelatase lead to erythropoietic protoporphyria. *Blood.* 2000;96(4):1545-1549.
18. Dailey HA, Dailey TA, Wu CK, et al. Ferrochelatase at the millennium: structures, mechanisms and [2Fe-2S] clusters. *Cell Mol Life Sci.* 2000; 57(13):1909-1926.
19. Kim YM, Bergonia HA, Muller C, Pitt BR, Watkins WD, Lancaster JR Jr. Loss and degradation of enzyme-bound heme induced by cellular nitric oxide synthesis. *J Biol Chem.* 1995;270(11): 5710-5713.
20. Sellers VM, Johnson MK, Dailey HA. Function of the [2FE-2S] cluster in mammalian ferrochelatase: a possible role as a nitric oxide sensor. *Biochemistry.* 1996;35(8):2699-2704.
21. Furukawa T, Kohno H, Tokunaga R, Taketani S. Nitric oxide-mediated inactivation of mammalian ferrochelatase in vivo and in vitro: possible involvement of the iron-sulphur cluster of the enzyme. *Biochem J.* 1995;310(2):533-538.
22. Taketani S, Adachi Y, Nakahashi Y. Regulation of the expression of human ferrochelatase by intracellular iron levels. *Eur J Biochem.* 2000;267(15): 4685-4692.
23. Mochel F, Knight MA, Tong WH, et al. Splice mutation in the iron-sulfur cluster scaffold protein ISCU causes myopathy with exercise intolerance. *Am J Hum Genet.* 2008;82(3):652-660.
24. Olsson A, Lind L, Thornell LE, Holmberg M. Myopathy with lactic acidosis is linked to chromosome 12q23.3-24.11 and caused by an intron mutation in the ISCU gene resulting in a splicing defect. *Hum Mol Genet.* 2008;17(11):1666-1672.
25. Kina T, Ikuta K, Takayama E, et al. The monoclonal antibody TER-119 recognizes a molecule associated with glycophorin A and specifically marks the late stages of murine erythroid lineage. *Br J Haematol.* 2000;109(2):280-287.
26. Shepherd M, Dailey TA, Dailey HA. A new class of [2Fe-2S]-cluster-containing protoporphyrin (IX) ferrochelatases. *Biochem J.* 2006;397(1):47-52.
27. Jones MS, Jones OT. The structural organization of haem synthesis in rat liver mitochondria. *Biochem J.* 1969;113(3):507-514.
28. Li FM, Lim CK, Peters TJ. An HPLC assay for rat liver ferrochelatase activity. *Biomed Chromatogr.* 1987;2(4):164-168.
29. Falk JE. *Porphyrins and Metalloporphyrins: Their*

General, Physical and Coordination Chemistry, and Laboratory Methods. Amsterdam, The Netherlands: Elsevier; 1964.

30. Crooks DR, Ghosh MC, Braun-Sommargren M, Rouault TA, Smith DR. Manganese targets m-aconitase and activates iron regulatory protein 2 in AF5 GABAergic cells. *J Neurosci Res.* 2007; 85(8):1797-1809.
31. Livak KJ, Schmittgen TD. Analysis of relative gene expression data using real-time quantitative PCR and the 2(-delta delta C(T)) method. *Methods.* 2001;25(4):402-408.
32. Tong WH, Rouault TA. Functions of mitochondrial ISCU and cytosolic ISCU in mammalian iron-sulfur cluster biogenesis and iron homeostasis. *Cell Metab*. 2006;3(3):199-210.
33. Bonifacino JS, Dell'Angelica EC, Springer TA. Immunoprecipitation. *Curr Protoc Protein Sci.* 2001;Chapter 9:Unit 98.
34. Shoubridge EA, Johns T, Boulet L. Use of myoblast cultures to study mitochondrial myopathies. *Methods Enzymol*. 1996;264:465-475.
35. Anguita E, Hughes J, Heyworth C, Blobel GA, Wood WG, Higgs DR. Globin gene activation during haemopoiesis is driven by protein complexes nucleated by GATA-1 and GATA-2. *EMBO J.* 2004;23(14):2841-2852.
36. Chan RY, Schulman HM, Ponka P. Expression of ferrochelatase mRNA in erythroid and non-erythroid cells. *Biochem J.* 1993;292(2):343-349.
37. Lake-Bullock H, Dailey HA. Biphasic ordered induction of heme synthesis in differentiating murine erythroleukemia cells: role of erythroid 5-aminolevulinate synthase. *Mol Cell Biol.* 1993; 13(11):7122-7132.
38. Powis G. Metabolism and reactions of quinoid anticancer agents. *Pharmacol Ther.* 1987;35(1): 57-162.
39. Nilsson R, Schultz IJ, Pierce EL, et al. Discovery of genes essential for heme biosynthesis through large-scale gene expression analysis. *Cell Metab.* 2009;10(2):119-130.
40. Gelling C, Dawes IW, Richhardt N, Lill R, Muhlenhoff U. Mitochondrial Iba57p is required for Fe/S cluster formation on aconitase and activation of radical SAM enzymes. *Mol Cell Biol.* 2008;28(5):1851-1861.
41. Wingert RA, Galloway JL, Barut B, et al. Deficiency of glutaredoxin 5 reveals Fe-S clusters are required for vertebrate haem synthesis. *Nature.* 2005;436(7053):1035-1039.
42. Jensen LT, Culotta VC. Role of *Saccharomyces cerevisiae* ISA1 and ISA2 in iron homeostasis. *Mol Cell Biol.* 2000;20(11):3918-3927.
43. Magness ST, Tugores A, Brenner DA. Analysis of ferrochelatase expression during hematopoietic development of embryonic stem cells. *Blood.* 2000;95(11):3568-3577.
44. Hall RE, Henriksson KG, Lewis SF, Haller RG, Kennaway NG. Mitochondrial myopathy with succinate dehydrogenase and aconitase deficiency: abnormalities of several iron-sulfur proteins. *J Clin Invest.* 1993;92(6):2660-2666.
45. Larsson LE, Linderholm H, Mueller R, Ringqvist T, Soernaes R. Hereditary metabolic myopathy with paroxysmal myoglobinuria due to abnormal glycolysis. *J Neurol Neurosurg Psychiatry.* 1964; 27:361-380.
46. Guillon B, Bulteau AL, Wattenhofer-Donze M, et al. Frataxin deficiency causes upregulation of mitochondrial Lon and ClpP proteases and severe loss of mitochondrial Fe-S proteins. *FEBS J.* 2009;276(4):1036-1047.
47. Puccio H, Koenig M. Friedreich ataxia: a paradigm for mitochondrial diseases. *Curr Opin Genet Dev.* 2002;12(3):272-277.
48. Bayot A, Basse N, Lee I, et al. Towards the control of intracellular protein turnover: mitochondrial Lon protease inhibitors versus proteasome inhibitors. *Biochimie.* 2008;90(2):260-269.
49. Kollberg G, Tulinius M, Melberg A, et al. Clinical manifestation and a new ISCU mutation in iron-sulphur cluster deficiency myopathy. *Brain*. 2009; 132(8):2170-2179.